Evaluation of Network Real Time Kinematics contribution to the accuracy/productivity ratio for UAS-SfM Photogrammetry

S. PANAGIOTOPOULOU[*], A. ERKEKI[*], A. ANTONAKAKIS[*], P. GRIGORAKAKIS[*], V. PROTOPAPA[*], G. TSIOSTAS[*], K. VLACHOU[*] & EMM. VASSILAKIS[**]

[*]Metrica SA
Athens, GREECE
email: s.panagiotopoulou@metrica.gr
email: a.erkeki@metrica.gr
email: a.antonakakis@metrica.gr
email: p.grigorakakis@metrica.gr
email: v.protopapa@metrica.gr
email: g.tsiostas@metrica.gr
email: k.vlachou@metrica.gr

[**]National and Kapodistrian University of Athens, Faculty of Geology and Geoenvironment, Remote Sensing Laboratory, Athens, GREECE
email: evasilak@geol.uoa.gr

Abstract: *The improvement of the accuracy of Structure-from-Motion photogrammetric products is discussed in this paper. In most cases it depends on the number and distribution of ground control points (GCPs) for block orientation, although the placement and precise measuring of GCPs are often time-consuming in a UAS project. This paper presents the evaluation of two approaches including Post Process Kinematic (PPK) and Network Real Time Kinematic (NRTK) methods aiming to avoid GCPs establishment, taking advantage of a real time positioning service, where differential corrections are sent from a network of Reference stations directly to the UAS.*

Keywords: UAS, AT, DG, CP, GCP, PPK, GNSS, NRTK

1. Introduction

The last few years, unmanned aerial systems (UASs), have become a popular tool for acquiring reliable survey data in environmental monitoring, construction, surveying, mining, and safety [1]. Lately, these industries use aerial imagery and through photogrammetric processing valuable insights from large data sets are generated, making it possible to see and measure the open surface changes that occur over time on work sites, mines and properties [2]. Also, they add valuable contribution on mapping of hard-to-access, hazardous or/and GNSS-denied parts of the areas of interest. As widely acknowledged, remote sensing techniques always provide an alternative and fully operational solution at such cases but lately UASs provide high resolution, reliable, on-demand data with higher temporal flexibility in comparison to any other satellite optical data [3]. However, traditional georeferencing of imagery acquired by UAS called aerial triangulation (AT), through photogrammetric procedures, involves the use of measured ground control points (GCPs)[4], which is a time consuming job and generally represents a negative factor for efficient mapping in remote and inaccessible areas. The number of GCPs obtained improve the accuracy of the final photogrammetric product, although, as it is generally accepted at least three GCPs are necessary for the process of georeferencing [5-6].

Many studies conducted to research the number and distribution of ground control points that are necessary in order to achieve high precision results [7-12]. The latest development of Direct Georeferencing (DG) of imagery captured by UASs [13-16] not require Ground Control Points which reduce time on field by the direct measurements of the absolute camera positions and altitudes using an on board Global Navigation Satellite System (GNSS) receiver, antenna and inertial measurement unit (IMU) and can achieve high accuracy on spatial data compared to data acquisition with the use of GCPs. The direct position and orientation measurements of the camera during the image acquisition, called Direct Geo-referencing (DG) [17-18], results a geo-referenced image to the given coordinate system without the need for any other ground information, in contrast to AT. This is made possible by taking advantage of the on-board GNSS receivers either in RTK or NRTK mode which increases the precision of the drone's position at the time of each image acquisition. The aforementioned equipment is available on several affordable UASs that exist in the market mainly focusing on the speeding-up of data acquisition during the fieldwork and thus making it more productive [19-20].

The experiment described in this work performed by using exclusively the novel DJI Phantom 4 RTK, which with the onboard multi-frequency multi-constellation GNSS receiver, fulfills the technological equipment mentioned above [21]. This allowed the adoption of NRTK (Network Real-Time Kinematic) and PPK (Post-Processed Kinematic) approaches for the data processing. The main objective of this experiment was to evaluate the geospatial accuracy of imagery products generated from UAS data photogrammetric processing, in an area with no complicated relief, by correcting the camera positions with three different methodologies.

2. Study Area and Data acquisition

The coastal area of Psatha Bay was chosen as the study area, initially because of its sufficient base station coverage and secondly because of the land cover variability. It is a provincial touristic area located at the easternmost shoreline of the Corinth Gulf, which is one of the most active rifts of the globe. Several geomorphological structures can be identified within a 3 km^2 area, including an extensive coble beach, a marshland of approximately 0.8 km^2, which has been developed upstream the coastal zone (Fig. 1). All the above are being placed in between two cliff coasts consisting of Mesozoic limestones [22]. The southernmost 200 m high cliff represents an almost vertical scarp comprising the footwall of the highly active seismic fault of Psatha. Along the base of the cliff, three uplifted marine solution notches have been developed corresponding to former sea - levels and indicating tectonic uplift of the area, which reaches a rate of the order of 0.3 mm/year for the last 10 kyr [23]. On the hanging wall of the fault a talus scree slope is developed with rocky material detached from higher altitudes. It seems that most of the debris were removed from the hanging wall during the last two decades, as the slope was used as an improvised quarry for building material.

The changes along the escarpment are impressive as the overall elevation change was quantified and at certain areas the total soil loss exceeded the 80 meters caused either by erosion or human interference.

Therefore, it is clear that the study area is a quite challenging one with complicated geomorphology, ideal for getting objectivity out of our experiment.

Figure 1: Index map of the study area of Psatha (right) and its location within Greece (left) and Corinth Gulf (middle).

3. Material and Methods

The aerial operations performed with the use of an RTK multi-copter the DJI Phantom 4 Pro RTK (DJI-P 4 RTK), which is equipped with a 20 MPix camera and high-precision multi-frequency GNSS receiver which is able to receive GPS, GLONASS, Galileo, and Beidou signals. The addition of the GNSS receiver enables the use of RTK module achieving centimeter-level accuracy with the latter one has made coastal mapping with direct georeferencing less challenging and equally precision wise with AT traditional method. The flight route is continuously recorded in real time during each automatic flight operation, and the GNSS observations are stored into a RINEX file v.3.03 with a sampling rate 5Hz. Whenever an image is captured by the camera of the DJI-P4RTK on a mission, a GNSS timestamp (in terms of GNSS Week and Time of Week) is also recorded[24].

The ortho-photo mosaics, dense point clouds and Digital Elevation models were generated with the commercial software (Agisoft Metashape, Professional Edition 1.6.3, Agisoft LLC, St. Petersburg, Russia[25]) which performs automatic tie point extraction and feature matching with bundle block adjustment (BBA) [26]. The software is based on the structure from motion (SfM) algorithms [27-28].

The area of interest extends at almost 0.8 km^2 and was covered with 2-3 flights depending on the batteries power-load and the weather conditions during each flight (wind speed and direction). The entire flight and the density of the photos were conformed due to this time limit. The high resolution natural color images were collected by its built in camera, installed on a two-axis gimbal. The photos were taken at an relative elevation of 85 meters above take off location, in E-W direction crosswise to the long axis of the coastal area, with 75% forward and side overlap, aiming to a ground sample distance (GSD) of 2.5 cm/pix. The DJI Phantom 4 RTK UAV uses the WGS84 coordinate system for flight navigation and geotagging the image files. The GNSS (single frequency receiver C/A, L1) UAS flight data were saved in an onboard LOG file.

More than a thousand of aerial images were acquired during each flight and they were processed through photogrammetric software in order to produce micro-topography and high resolution mosaic imagery. Eight (8) Ground Control Points (GCPs) were ideally spread at different elevations around the area and measured with a high precision dual-frequency GNSS receiver Hi Target iRTK5 in order to maximize the accuracy of each processing, since a comparative study was the main objective [29]. The points were used as ground control or as check points within the photogrammetric processing, were established and measured by NRTK with the real-time positioning service HxGN SmartNet of Greece (HxGN SmartNet, https://www.metrica.gr/smartnet-greece) and the accuracies achieved were ±1–1.5 cm in horizontal coordinates and ±1.6–3 cm in elevation [30].

The photogrammetric procedure started with aligning the aerial images and creating a sparse 3D point cloud followed by a mesh generation. Following locating the GCPs on every image and inserting the exact coordinates and elevation measured by the RTK GNSS was the next step in the methodology (depending on the requirements of each experiment phase), which is the recommended photogrammetric procedure outlined by Agisoft Metashape commercial software and was slightly modified for reducing geometry errors and constructing the dense point cloud. The generation of ortho-photo-mosaics and DSMs complete the procedure (Fig. 2).

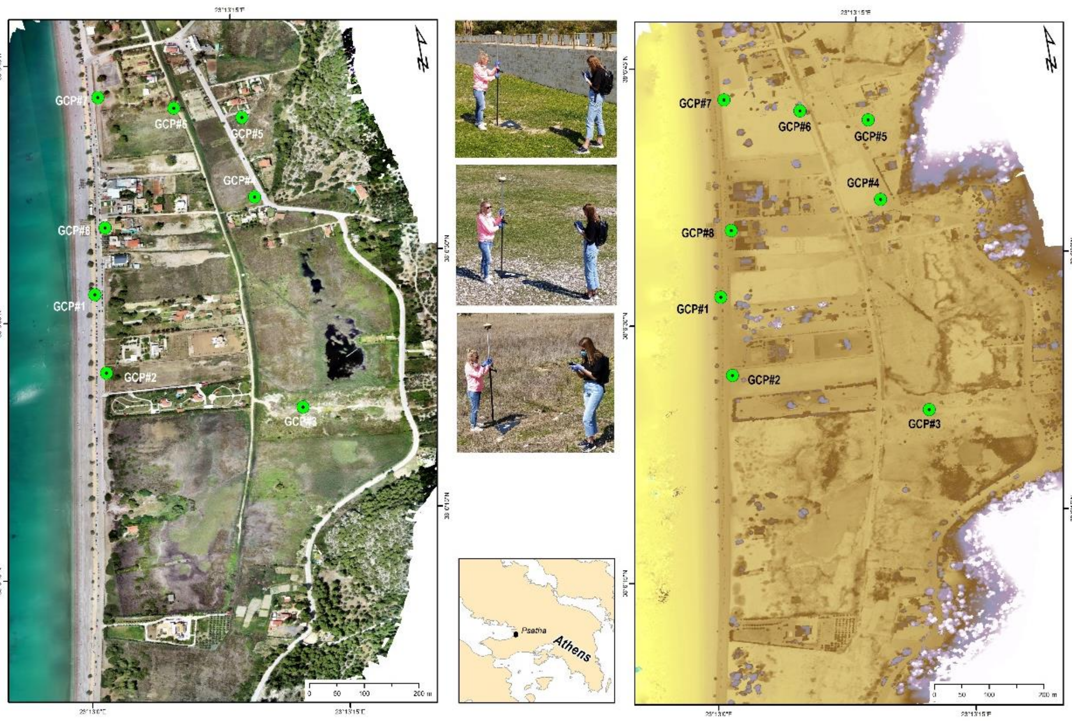

Figure 2. The area of the experiment represented by an ortho-photo-mosaic (left) and a Digital Surface Model (right). The ground points' locations are presented as well as some photographs during the field measurements with a RTK-GNSS receiver. The inset at the center below shows the area location west of Athens.

The image acquisition was repeated three times with different settings for the needs of the described experiment. At the first set of images, the UAS was used without any location control other than the built in GNSS receiver. The flight is performed adopting the conventional approach, and the positioning is demanded to the onboard GNSS receiver but without any correction applied. The measured ground points were used as GCPs during the photogrammetric processing and the result was satisfactory succeeding error on 3D of the order of ±6.5 cm (See Table 3).

The second set of images was acquired by using the HxGN SmartNet reference stations for Network Real Time Kinematic (NRTK) solution using VRS and NEAR network solutions of the RTK UAS image capturing locations. Within this approach the UAS is connected via the Internet Protocol NTRIP through the radio controller device and can download the needed corrections from a network of base stations. In order to achieve that a part of the highly accurate Greek continuously operating reference stations network (HxGN SmartNet of Greece) was used (Fig. 3). A continuously measuring GNSS station network provided optimal correction data for real time measurements which obtained the reading at the centimeter level via GPS, GLONASS, Galileo and BeiDou. The UAS was used as a rover antenna connecting with the CORS network HxGN SmartNet in Greece via Internet Protocol (NTRIP) where during its flights and therefore the camera positions were corrected in real time [31-33] . The difference of DG with AT approach, is the direct georeferencing of images where with direct calculation of the camera orientation and position each pixel is georeferenced to the wanted ground coordinate reference system without any measured ground control point. The acquired images were imported in the Agisoft Metashape workflow and the photogrammetric processing was completed without including any GCP location information. In this case the measured points were used as validation points for comparing the outcome of this current photogrammetric processing and control its quality (to validate the accuracy of the model reconstruction to evaluate the georeferenced to the target coordinate system ETRS89, ETRF2005 (t=2007.5)).

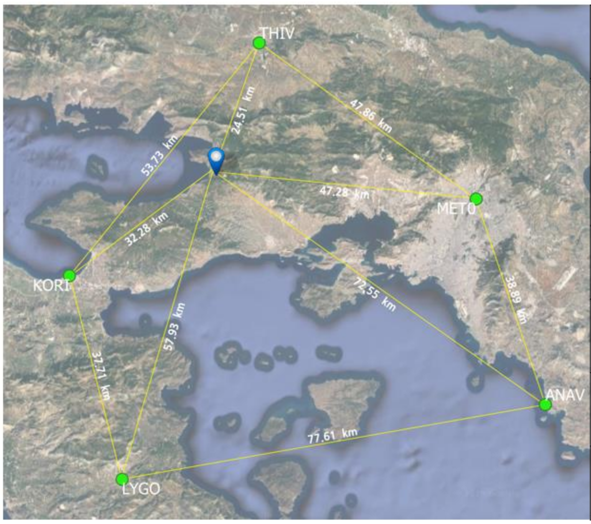

Coordinates in GGRS87			
	E (m)	N(m)	H(m)
ANAV	491400,762	4175948,265	17,704
KORI	405913,565	4199583,420	18,914
LYGO	414916,574	4162970,443	356,739
MET0	479000,630	4212795,620	181,288
THIV	440263,753	4240870,895	223,282

Figure 3: Location of study area and nearby reference stations of HxGN SmartNet Greece.

The last image data acquisition performed with the traditional approach with RTK method but post processed after the field work using the differential correction data from the Reference Station (KORI, Ref. Station ID 0002) provided by HxGN SmartNet. Its solution was used for Post Processing of the UAS image capturing locations, since it was collecting and storing RINEX data throughout the entire flight duration. The UAS camera positions were recalculated after post processing and followed the Agisoft Metashape workflow for generating an ortho-photo-mosaic without including any GCP information.

The ground points were used as check points in this case, as well, succeeding accuracy in the order of EN 4.9 cm and 6.4 cm on U component, (See Table 2). At the new image product, we located the GCPs, measured the coordinates on the screen and used them for comparison with the results generated from the other two methods.

4. Results

In order to compare the results for all different approaches GCPs used as CPs and the comparison focused on the coordinates measured on the field from NRTK with the GNSS receiver and the coordinates estimated after the photogrammetric procedure for each dataset.

i. GCPs

CP	ΔE (m)	ΔN (m)	ΔH (m)	3D (m)
1	-0.005	0.021	-0.034	0.040
2	-0.002	0.024	0.002	0.024
3	0.014	-0.004	0.009	0.017
4	0.020	0.001	-0.005	0.021
5	0.038	-0.003	-0.088	0.096
6	0.057	-0.006	0.081	0.099
7	-0.073	-0.046	-0.039	0.095
8	-0.045	0.011	0.030	0.055
Mean	**0.032**	**0.014**	**0.036**	**0.056**
Std.Dev.	0.026	0.015	0.033	0.036
	RMSe E (m)	RMSe N (m)	RMSe U (m)	RMSe 3D (m)
8 CPs (1-8)	0.040	0.020	0.047	**0.065**

Table 1. Comparison between reference coordinates of CPs and coordinates estimated using AT UAV method with the use of 8 GCPs.

ii. PPK

For the dataset obtained from the post process kinematic witht he use of the base station D-RTK2 as reference the RMSE on the total of CPs reported in Table 1 and on Table 2 the residuals for each of check point.

CP	ΔE (m)	ΔN (m)	ΔH (m)	3D (m)
1	-0,006	0,023	0,061	0,030
2	-0,023	0,002	0,061	0,029
3	-0,038	-0,039	0,074	0,084
4	0,041	-0,003	-0,025	0,023
5	-0,044	-0,036	0,034	0,038
6	0,011	-0,075	0,057	0,048
7	-0,038	-0,128	-0,081	0,082
8	-0,074	0,014	-0,091	0,059
Mean	0,034	0,040	0,060	0,049
Std.Dev.	0,021	0,042	0,022	0,024
	RMSe E (m)	RMSe N (m)	RMSe U (m)	RMSe 3D (m)
8 CPs (1-8)	0,040	0,055	0,064	**0,054**

Table 2. Comparison between reference coordinates of CPs and coordinates estimated using PPK UAV positioning method.

iii. NRTK

CP	ΔE (m)	ΔN (m)	ΔH (m)	3D (m)
1	0,050	0,090	-0,096	0,079
2	-0,017	0,042	-0,064	0,041
3	-0,004	0,007	-0,089	0,033
4	-0,033	-0,092	-0,120	0,082
5	-0,049	-0,056	-0,129	0,078
6	-0,032	-0,032	-0,146	0,070
7	-0,069	-0,041	--0,128	0,080
8	-0,049	-0,038	0,134	0,074
Mean	-0,038	-0,050	-0,113	0,067
Std.Dev.	0,021	0,029	0,028	0,019
	RMSe E (m)	RMSe N (m)	RMSe U (m)	RMSe 3D (m)
8 CPs (1-8)	0,043	0,057	0,116	**0,069**

Table 3. Comparison between reference coordinates of CPs and coordinates estimated using DG NRTK UAV method.

5. Conclusions

Three methodologies for extracting high accuracy ortho-photo-mosaics were briefly described in this paper. The GCP method can obtain accuracy from survey grade precision and transfer this into the photogrammetric software workflow. However, despite the high accuracy that this method may offer, the amount of time spent during the fieldwork (for selecting and measuring each GCP), as well as afterwards in the laboratory (for using markers in the projects by locating the GCPs at every image), could make this method unproductive and cost effectiveness depending on the project size and the terrain. During the PPK method the corrections were applied post-flight at the laboratory and obtained accuracy, which was transferred after the post processing correction for each camera position. This method was clearly more accurate since it is depended on the high accuracy HxGN SmartNet service, not to mention that significant amount of fieldwork time is saved. The NRTK method seems to be the most appropriate not only precision-wise as succeeded similar accuracy with GCP approach but also time-wise, considering that the UAS GNSS receiver can continuously communicate with the base station in real time and corrections can be simultaneously applied during the flight with the use of the HxGN SmartNet service. The accuracies obtained using a reference base station with PPK comparing to NRTK presented minor EN differences, which yield that the latter is more productive as it can be less time consuming.

References

[1] D. Giordan, Y. Hayakawa, F. Nex, F. Remondino, P. Tarolli,. Review article: the use of remotely piloted aircraft systems (RPASs) for natural hazards monitoring and management Nat Hazards *Earth Syst Sci* 18, 2018:1079-1096 doi:10.5194/nhess-18-1079-2018

[2] E. Vassilakis, M. Foumelis, A. Erkeki, E. Kotsi, I. Parcharidis, and E. Lekkas. Multitemporal Surface Deformation Analysis of Amyntaio Slide (Greece) using Remotely Piloted Airborne System and Structure-from-Motion photogrammetry. *4th Joint International Symposium on Deformation Monitoring*: 2019, Athens, p. 5p.

[3] E. Karantanellis, V. Marinos, E. Vassilakis, B. Christaras. Object-Based Analysis Using Unmanned Aerial Vehicles (UAVs) for Site-Specific Landslide Assessment: *Remote Sensing*. 2020, v. 12, no. 11, p. 1711

[4] Y. Taddia, F. Stecchi, A. Pellegrinelli. Coastal Mapping Using DJI Phantom 4 RTK in Post-Processing Kinematic Mode. *Drones* 2020,*4*, 9.

[5] F. Agüera-Vega, F. Carvajal-Ramírez, P. Martínez-Carricond. Assessment of photogrammetric mapping accuracy based on variation ground control points number using unmanned aerial vehicle. *Measurement*. 98. 10.1016/j.measurement.2016.12.002.

[6] G. Forlani, E. Dall'Asta, F. Diotri, , U.M di Cella., R. Roncella, M. Santise. Quality assessment of DSMs produced from UAV flights georeferenced with On-Board RTK positioning. Remote Sensing, 2018, 10. 311. 10.3390/rs10020311.

[7] E. Ferrer-González, F. Agüera-Vega, F. Carvajal-Ramírez, P. Martínez-Carricondo. UAV Photogrammetry Accuracy Assessment for Corridor Mapping Based on the Number and Distribution of Ground Control Points. *Remote Sensing,* 2020, 12, 2447.

[8] E. Stott, R.D. Williams, T.B. Hoey. Ground Control Point Distribution for Accurate Kilometre-Scale Topographic Mapping Using an RTK-GNSS Unmanned Aerial Vehicle and SfM Photogrammetry. *Drones* **2020**, *4*, 55.

[9] F. Agüera-Vega, F. Carvajal-Ramírez, P. Martínez-Carricondo. Assessment of photogrammetric mapping accuracy based on variation ground control points number using unmanned aerial vehicle. *Measurement*, 2017 98. 10.1016/j.measurement.2016.12.002.

[10] K.N. Tahar. An evaluation on different number of ground control points in unmanned aerial vehicle photogrammetric block. *ISPRS - International Archives of the Photogrammetry, Remote Sensing and Spatial Information Sciences*, 2013. XL-2/W2. 93-98. 10.5194/isprsarchives-XL-2-W2-93-2013.

[11] L.L. Teppati, F. Chiabrando, F. G. Tonolo. ARE MEASURED GROUND CONTROL POINTS STILL REQUIRED IN UAV BASED LARGE SCALE MAPPING? ASSESSING THE POSITIONAL ACCURACY OF AN RTK MULTI-ROTOR PLATFORM, Int. Arch. Photogram. Remote Sens. Spatial Inf. Sci., 2020, XLIII-B1-2020, 507–514, https://doi.org/10.5194/isprs-archives-XLIII-B1-2020-507-2020,.

[12] V.E. Oniga, A.I. Breaban, F. Statescu. Determining the Optimum Number of Ground Control Points for Obtaining High Precision Results Based on UAS Images. *Proceedings*, 2018, 2, 352. DOI:10.3390/ecrs-2-05165.

[13] B. Grayson, N.T. Penna, J.P. Mills, D.S. Grant. GPS precise point positioning for UAV photogrammetry. *The Photogrammetric Record*, 2018, 10.1111/phor.12259.

[14] L. Klingbeil, C. Eling, E. Heinz, M. Wieland, H. Kuhlmann. Direct georeferencing for portable mapping systems: In the air and on the ground. *Journal of Surveying Engineering*, 2017, 143. 04017010. 10.1061/(ASCE)SU.1943-5428.0000229.

[15] M.J. Westoby, J. Brasington, N.F. Glasser, Hambrey, M.J., J.M. Reynolds. Structure-from-Motion photogrammetry: A low-cost, effective tool for geoscience applications. *Geomorphology*, 2012179:300-314 doi:10.1016/j.geomorph.2012.08.021

[16] P. Heinz-Jürgen & B. Manfred. RTK and PPK: GNSS-Technologies for direct georeferencing of UAV image flights. *FIG Working Week*,2020, Netherlands.

[17] A. Zanutta, A. Lambertini, L. Vittuari. UAV Photogrammetry and Ground Surveys as a Mapping Tool for Quickly Monitoring Shoreline and Beach Changes. *Journal of Marine Science and Engineering*, 2020, 8. 52. 10.3390/jmse8010052.

[18] M. Rabah, M. Basiouny, E. Ghanem & A. Elhadary. Using RTK and VRS in direct geo-referencing of the UAV imagery, *NRIAG Journal of Astronomy and Geophysics*, 2018, 7:2, 220-226, DOI: 10.1016/j.nrjag.2018.05.0

[19] Y. Taddia, F. Stecchi, A. Pellegrinelli. Coastal Mapping Using DJI Phantom 4 RTK in Post-Processing Kinematic Mode. *Drones* 2020,*4*, 9.

[20] Y. Taddia, F. Stecchi, A. Pellegrinelli. USING DJI PHANTOM 4 RTK DRONE FOR TOPOGRAPHIC MAPPING OF COASTAL AREAS. *ISPRS - International Archives of the Photogrammetry, Remote Sensing and Spatial Information Sciences*, 2019, XLII-2/W13. 625-630. 10.5194/isprs-archives-XLII-2-W13-625-2019.

[21] DJI, Phantom 4 RTK User Manual, v2.4 DJI: Shenzhen, China

[22] J. Alexopoulos, E. Vassilakis, S. Dilalos, E. Zaloumi. Quantification of anthropogenic impact on natural evolution processes at a coastal zone, adjacent to an active fault. In: *13th International Conference on Environmental Science and Technology*, 2013, Athens.

[23] I. Mariolakos, I. Fountoulis. Quaternary repeated activity of the Psatha fault (Gulf of Corinth, Greece). *In abstracts of XVI Congress of Carpathian-Balkan Association, Vienna,* August 1998, Abstract, p. 366

[24] E. Stott, R.D. Williams, T.B. Hoey. Ground Control Point Distribution for Accurate Kilometre-Scale Topographic Mapping Using an RTK-GNSS Unmanned Aerial Vehicle and SfM Photogrammetry. *Drones* **2020**, *4*, 55.

[25] Agisoft LLC. Agisoft metashape user manual, Professional edition, Version 1.6, Agisoft LLC, St. Petersburg, Russia, Retrieved 6/1/2020, https://www.agisoft.com/pdf/metashape-pro_1_6_en.pd.

[26] S. Ullman. The interpretation of structure from motion. *Proc. R. Soc. Lond*. B 1979, 203, 405–426.

[27] M.J. Westoby, J. Brasington, N.F. Glasser, Hambrey, M.J., J.M. Reynolds. Structure-from-Motion photogrammetry: A low-cost, effective tool for geoscience applications. *Geomorphology*, 2012, 179:300-314 doi:10.1016/j.geomorph.2012.08.021

[28] S.I. Granshaw. Structure from motion: origins and originality. *The Photogrammetric Record*, 2018, 33:6-10 doi:10.1111/phor.12237

[29] D. Fugazza, M. Scaioni, M. Corti, C. D'Agata, R.S. Azzoni, M. Cernuschi, Smiraglia, C. A. Diolaiuti. Combination of UAV and terrestrial photogrammetry to assess rapid glacier evolution and map glacier hazards. *Nat. Hazards Earth Syst. Sci*., 2018, 18, pp. 1055-1071

[30] T. Baybura, İ. Tiryakioğlu, M. A. Uğur, H. İ. Solak, and Ş. Şafak. Examining the Accuracy of Network RTK and Long Base RTK Methods with Repetitive Measurements. *Journal of Sensors*, 2019, vol. 2019, Article ID 3572605, 12 pages.

[31] B. Tae-Suk, K. Minho. Performance Analysis of Network-RTK Techniques for Drone Navigation considering Ionospheric Conditions, *Journal of Sensors*, 2018, Article ID 5154697, 8 pages, 2018. https://doi.org/10.1155/2018/5154697.

[32] G. Hu, K. Khoo P., Goh, C. Law. Internet-based GPS VRS RTK positioning with a multiple reference station network. *Journal of Global Positioning Systems*, 2002, 1. 113-120. 10.5081/jgps.1.2.113.

[33] C. Rizos, S. Han. Reference station network based RTK systems-concepts and progress. Wuhan Univ. J. Nat. Sci., 2003, 8, 566–574. https://doi.org/10.1007/BF02899820